ECASIA special issue paper

SURFACE and INTERFACE ANALYSIS

Received: 2 September 2015 Revised: 26 February 2016 Accepted: 29 February 2016 Published online in Wiley Online Library: 4 April 2016

(wileyonlinelibrary.com) DOI 10.1002/sia.6010

# XPS investigations of graphene surface cleaning using $H_2$- and $Cl_2$-based inductively coupled plasma

D. Ferrah,[a,b,c]* O. Renault,[a,b] C. Petit-Etienne,[a,c] H. Okuno,[a,d] C. Berne,[a,e] V. Bouchiat[a,e] and G. Cunge[a,c]

**It is known that graphene surface contaminations by residues affect drastically its intrinsic properties and cannot be avoided when chemical vapor deposited (CVD) graphene is transferred on other substrates. In this work, we investigate by X-ray photoelectron spectroscopy and work function measurements using X-ray photoemission electron microscopy the capabilities of high-density plasmas to clean graphene. The evolution of different chemical species at surface is monitored as a function of plasma exposure. $H_2$ plasmas are shown to clean efficiently PMMA residues from CVD graphene on Cu. However, when the same plasma is used on graphene transferred on $SiO_2$/Si substrate a *liftoff* of the graphene layer is observed before the end of cleaning procedure. These results are discussed in terms of $H^+$ penetration through graphene and $H_2$ formation between the $SiO_2$ substrate and graphene. Using Cl-based chemistries, we found that the plasma is able to etch polymeric contamination at the graphene surface. It is also found that the plasma induces spreading of the Si nanoparticle contamination that hampers the cleaning process.**


**Keywords:** dry-cleaning; graphene; photoelectron spectroscopy; photoemission electron microscopy; work function

## Introduction

Graphene offers many exciting new technology applications owing to its unusual electronic properties.[1] For large-scale manufacturing of graphene in semiconductor device, large area and high-quality graphene film transferred onto various substrates is required. At the same time, it is also mandatory to develop efficient graphene treatment to clean the inevitable contamination that occurs in the manufacturing process (CVD growth, transfer and patterning), because this contamination degrades dramatically graphene properties.[2] Typical contaminants include organic resist residues originated from spin-coated polymer thin films,[3] usually poly (methylmethacrylate) (PMMA), used as a mechanical support to transfer graphene or as a photolithographic mask. In addition, Si-based nanoparticle impurity have been observed on CVD graphene and probably originate from CVD oven.[4,5] In recent years, effort to improve the cleanness of graphene has been made. In fact, various combinations of organic solvent rinses have been investigated[6] in an attempt to remove polymeric residues, but graphene always remains contaminated. Annealing under controlled atmosphere such as $H_2$/Ar[5,7] and $CO_2$[8,9] or a vacuum[10] has been explored and shows PMMA residues to be significantly reduced, but it leaves specific 2D polymeric layers at the surface of graphene as evidenced by transmission electron microscopy (TEM).[5] Elsewhere, mechanical cleaning of graphene based on the contact mode atomic microscopy removes residues and improves the electronic mobility without damaging graphene as reported by Goossens et al.[11] This cleaning procedure displays a higher carrier mobility of transferred graphene as reported in the literature but is not suitable for large areas as required for industry application. Furthermore, no or few interest has been payed to Si-based nanoparticles' impurity removal.[12]

Reactive plasma processes for cleaning and doping are used since years in the semiconductor industry, and they attract a growing interest to modify or clean graphene.[13–16] A recent study on the selective dry-etching mechanism of PMMA over single layer of CVD graphene on Cu foil in $H_2/N_2$ plasma[17] shows particularly promising results. The etching process has been achieved in a high-density plasma reactor that provides a low enough ion bombardment energy to prevent graphene damage. In this study, the mechanism of plasma/PMMA interaction was detailed and displays two distinct stages of PMMA etching: an initial stage with a fast etching rate corresponding to the removal of bulk $PMMA^B$ and a much slower stage corresponding to the removal of the PMMA at the interface. Indeed, a gradient in the PMMA layer density was observed on the ten last nanometers above the surface. These correspond to amorphous structures called $PMMA^A$ that are similar to

* *Correspondence to: D. Ferrah, CEA, LETI, Minatec Campus, F-38054 Grenoble, France.*
*E-mail: Djawhar.FERRAH@cea.fr*

a *Univ. Grenoble Alpes, F-38000, Grenoble, France*

b *CEA, LETI, Minatec Campus, F-38054, Grenoble, France*

c *LTM-CNRS, Minatec Campus, F-38054, Grenoble, France*

d *INAC-CNRS, Minatec Campus, F-38054, Grenoble, France*

e *Institut Néel, CNRS-UJF, BP 166, 38042, Grenoble cedex 9, France*

PMMA but denser and easily etched by the plasma and self-organized 2D structures called PMMA$^G$ at the graphene surface that are heavily oxidized. The latter are shown to be removed by a lateral (thus slow) etching mechanism by H atoms.

In this work, we have investigated the cleaning and limitation of hydrogen plasma process on CVD graphene transferred on $SiO_2$ on Si substrate. We also introduced chlorine plasma cleaning. This optimized new plasma does not appear to damage graphene that is in good agreement with previously published results.[18] To monitor chemical and local electronic surface modification after plasma treatment, X-ray photoelectron spectroscopy (XPS) and work function measurements using X-ray photoemission electron microscopy (X-PEEM) have been made.

## Experimental

Samples used in this study were obtained by transferring CVD graphene grown on Cu foil (monolayer with low percentage of multilayer coverage) on both $SiO_2$ (300 nm) on Si and $SiO_2$ (4 nm) on Si substrates by standard procedure using polymer layer (PMMA) as support. The thickness and the quality of the graphene were determined by Raman and SEM measurements. The $1 \times 1\ cm^2$ samples were stick on a 300-mm diameter alumina wafer using Kapton tape.

The samples were etched in a commercially available AdvantEdgeTM inductively coupled plasma (ICP) etch tool from Applied Materials, described in details in ref.[19] Usually, it is tricky to prevent the presence of parasitic species in reactive plasmas. These species originate from the erosion of the reactor walls, and the presence of O atoms must be precluded when etching graphene. We find that a convenient solution to reach this goal was to operate in a fully fluorinated chamber (obtained by running a $SF_6/O_2$ plasma in the chamber/carrier substrate). The resulting $AlF_3$ layer is stable and O free both in $H_2$ and $Cl_2$ plasmas.[20]

The plasma was operated at either 200 or 400 W radio frequency (rf) power. To ensure minimizing damages caused by energetic ion impacts, we operate the plasma at relatively high pressure, which minimizes both the ion flux and their energy. At 60 mTorr under our condition, the ion energy was measured to be in the 9–15 eV range. This caused the sample temperature to rise up to 120 °C. Operating at high pressure also ensures a high flux of reactive radicals to the wafer and thus a large etch rate.

XPS measurements over an area of few $mm^2$ were carried out at a base pressure $10^{-10}$ mbar in a Multiprobe spectrometer (ScientaOmicron) fitted with a Monochromatized Al $K_\alpha$ source (1486.6 eV) and a 128 channel, parallel detection Argus electron analyzer. The overall energy resolution was 270 meV. The emission angle is fixed to 20° with respect to the surface normal. Thus, the probed depth is about 8 nm for PMMA and graphene ($\lambda$ ~3 nm).[21,22] The spectrometer chamber is connected to a preparation chamber in which samples could be annealed in ultrahigh vacuum ($10^{-10}$ mbar) in order to remove chemisorbed impurities. XPS is a suitable technique to obtain insight into the chemical composition and the stoichiometry of the extreme surface after surface plasma treatment.

The X-PEEM experiments were made in ultra-high vacuum chamber using a NanoESCA spectromicroscope (ScientaOmicron), described previously elsewhere.[23] A double pass hemispherical energy analyzer was used to compensate single analyzer aberrations. The X-PEEM image series was acquired at the photoemission threshold region. A 68 μm field of view was used with 12 kV extraction voltage and about 1.8 mm sample-objective lens distance. The overall energy resolution of the analysis was 800 meV. A contrast aperture of 1500 μm was used corresponding to lateral resolution of about 1 μm. After correction for the Schottky effect of 98 meV because of the high extractor field, the fit of photoemission threshold spectra with error function can be used to directly measure the local work function. Then, the series of images taken at an increasing photoelectron kinetic energy enables us to determine work function map obtained from fit of spectrum for each pixel.

## Results and discussion

Figure 1 displays C1s core level spectra from CVD graphene on Cu foil and from the same CVD graphene but after transfer on a $SiO_2$ (300 nm) on Si substrate. In each case, the thick PMMA layer spun on graphene was removed by acetone, and then, the samples were treated with the hydrogen plasma for 20 and 40 s. The spectra were fitted using standard procedures, i.e. Shirley background subtraction and resolution into Doniach-Sunjic function for $sp^2$ graphene-related component and Voigt function for the other components. The C1s spectrum from CVD graphene on Cu before plasma treatment is reported in Fig. 1a. The solid curve that overlaps the observed spectrum is the contribution of six components. The main $sp^2$ component at 284.4 eV is attributed to a combination of both graphene and $sp^2$ coordinated amorphous carbon. The second $sp^3$ component at 285.0 eV is mainly assigned to amorphous carbon. The remaining four smaller C1s components (A) at 285.7 eV, (B) at 286.4 eV, (C) at 287.1 eV and (D) at 288.9 eV were assigned, respectively, to different chemical environments of carbon atoms in PMMA (C–H, C–C, H–C–O and O–C=O). The evolution of C1s spectrum after 20-s plasma exposure time shows a decrease in the intensity of PMMA components, as displayed in Fig. 1b. Additionally, oxidized carbon contributions in PMMA residues become important that appear as high binding energy components in C1s spectrum, namely C–O at 287.0 eV, C=O at 287.7 eV and O–C=O at 288.7 eV. This means that PMMA$^A$ residues are etched and heavily oxidized PMMA$^G$ residues start to be exposed to $H_2$ plasma.[17] Figure 1c shows that when plasma duration is increased to 40 s, there is no more PMMA residues remaining on graphene, but only two small components (in addition to $sp^2$) are identified: an $sp^3$ component attributed to pre-existing defects in CVD graphene, namely grain boundaries and/or structural vacancies or/and C–H bonds in hydrogenated graphene, and a second component located at 284.0 eV, which is attributed to graphene–Cu bonding at the interface and/or to presence of single vacancies.[24] This result demonstrates that $H_2$ plasma has the capability to clean CVD graphene on copper without irreversible damages (graphene hydrogenation is reversible by annealing). The PMMA etching mechanism has been described in detail in previous study.[17]

However, Fig. 1d, e and f shows that very different results are obtained when the same plasma treatment is applied to the same graphene but after its transfer from Cu foil to $SiO_2$ on Si substrate. Figure 1d and e shows that before and after plasma treatment for 20 s, there is only minor difference between CVD graphene on Cu foil or on $SiO_2$ on Si substrate. However, after 40 s of plasma treatment, as shown in Fig. 1f, there are no more graphene on the $SiO_2$ surface as evidenced by the disappearance of the $sp^2$ component. Other contributions from residues, namely $sp^3$, COH, CO and COO, are identified. This result is not in conflict with the CVD graphene on Cu cleaning, because the interface interaction between graphene and $SiO_2$ on Si is weaker than graphene and Cu. Indeed, dry-cleaning relies on H atoms that can react with PMMA

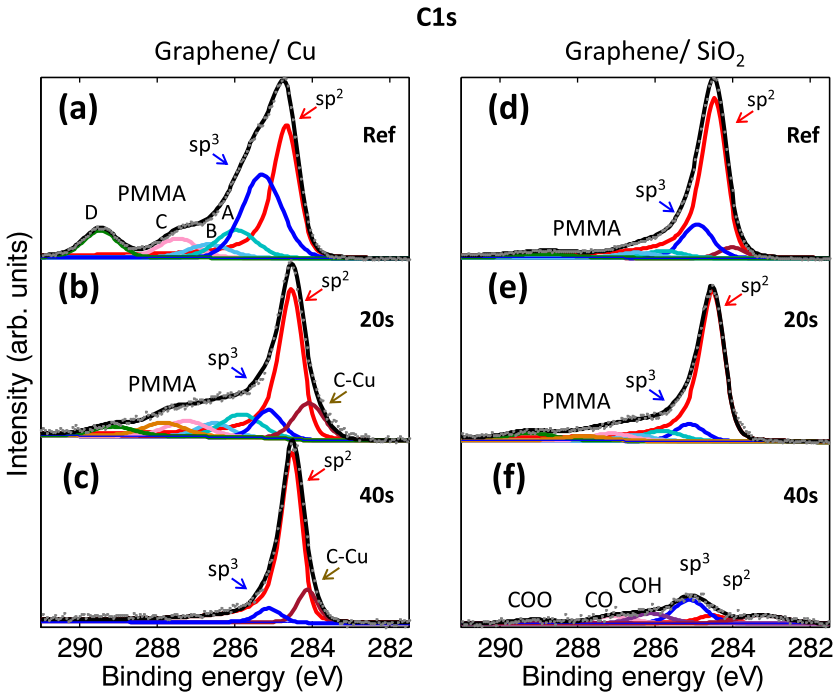


**Figure 1.** XPS C1s core level spectra (dots) obtained before and after 20 and 40 s of hydrogen plasma exposure, respectively: (a), (b) and (c) CVD graphene on Cu and (d), (e) and (f) CVD graphene transferred onto $SiO_2$ (300 nm) on Si samples. The solid curves show the contributions of graphene and PMMA in each spectrum.

to produce volatile species, such as CH or OH or $H_2O$. However, at the same time, the surface is bombarded by protons (and $H_x^+$ ions) whose energy is high enough to penetrate through the graphene lattice without damaging it.[25] The H atoms trapped between the substrate and graphene can recombine to form $H_2$ gas.[26] As a result, during the cleaning process, a gas forms between the $SiO_2$ and the graphene layer eventually leading to a liftoff of the layer when the trapped gas pressure overcomes the binding forces between graphene and the substrate. This is produced instantly about 30 s of plasma exposure time (refer Supplementary Material) that contradicts the graphene etching hypothesis and confirms the liftoff effect.

This phenomenon can be seen as an issue associated with the use of $H_2$ plasma to clean graphene. However, it should be possible to find plasma-operating conditions in which the ion flux and energy are small enough and the H atoms flux high enough to clean the PMMA residues before the liftoff mechanism is observed. This will be discussed in a forthcoming paper. Alternatively, one may think about using another gas to etch PMMA and to choose a plasma chemistry in which ions are too big to penetrate through graphene. We investigated $Cl_2$ plasmas for this reason, and the results are presented in the next section.

Figure 2 illustrates the impact of $Cl_2$ plasma process on CVD graphene transferred on $SiO_2$ (4 nm) on Si substrate. In order to remove the chemisorbed chlorine and its contributions in the C1s spectra, XPS measurements were carried out after vacuum annealing at 350 °C during 30 min. In Fig. 2a, the C1s spectra are decomposed into six components ($sp^2$, $sp^3$, A, B, C and D) as specified in the previous section. At lower binding energies, another new component at 283.9 eV is observed and attributed to C–Si bonds in PMMA. By contrast, the Si2p peak is more complex. The issue is that the observed silicon originates both from the $SiO_2$/c-Si substrate and from the $SiO_2$-coated Si nanoparticles that contaminate the graphene surface.[17] To investigate the different chemical environments of Si, Si2p spectra were decomposed by taking into account ($Si2p_{1/2}$ and $Si2p_{3/2}$) spin-orbit splitting of 0.6 eV and a branching ratio of 0.5.[27] Before plasma exposure, as shown in Fig. 2a, they were deconvoluted into six doublet components which main components ($Si2p_{3/2}$) are centered at 99.4 eV ($S_1$) assigned to Si from substrate, at 100 eV ($S_2$) assigned to Si from nanoparticles, at 100.3 eV ($S_3$) assigned to $Si_2O$ ($Si^+$), at 101.2 eV ($S_4$) assigned $Si_3O_2$ ($Si^{+2}$), at 102.2 eV ($S_5$) assigned to SiO ($Si^{+3}$) and at 103.7 eV ($S_6$) assigned to $SiO_2$ ($Si^{+4}$) from both substrate and nanoparticles. The contribution of Si–C bonds is identified in the $S_4$ component.

Firstly, according to $Cl_2$ plasma treatment for 40, 90, 140 and 220 s, C1s spectra show that the intensity of PMMA components (A, B, C and D) decreases after 40-s exposure time indicating a removal of PMMA from graphene. It shows, however, a decrease of overall C1s core level intensity from 40 s up to 160-s exposure time. These observations are not associated to liftoff or/and etching of the graphene layer in $Cl_2$ plasma, because after 160-s plasma exposure time, the C1s core level intensity hardly changes. Secondly, the Si2p spectra show an intensity increase and binding energy shift of $S_1$ and $S_6$ components associated to reorganization of $SiO_2$-coated Si nanoparticles at surface of graphene. The full binding energy shift reported after 220-s exposure time is 0.5 eV.

Figure 2b shows the intensity ratio evolutions of Si2p ($S_1$), Si2p ($S_2$), Si2p ($S_4$), Si2p ($S_6$) and C1s (Si–C) components to C1s ($sp^2$) component as function of plasma treatment duration. They mainly display two trends. With an exposure time up to 40 s, the intensity ratio of Si2p ($S_1$), Si2p ($S_2$) and Si2p ($S_6$) to C1s ($sp^2$) is decreasing indicating an increase of $sp^2$-related graphene component associated to PMMA removal from graphene. At the same time, the C–Si contribution in the C1s core level spectra increases rapidly and then saturates, which is indicating that silicon atoms from nanoparticles diffuse and react with the carbon from PMMA or graphene. This



  

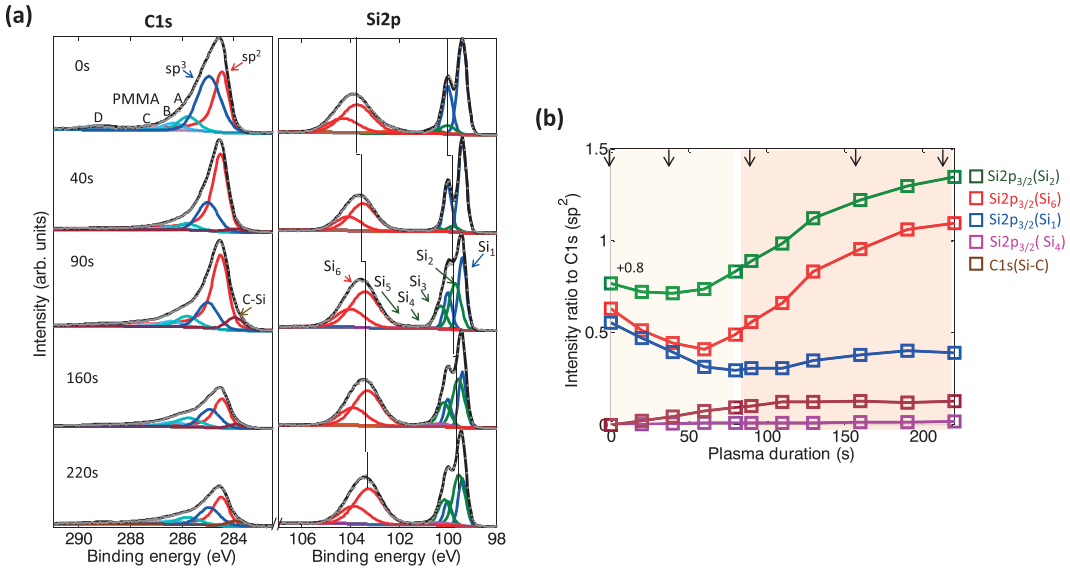


**Figure 2.** (a) XPS spectra of C1s and Si2p obtained on CVD graphene transferred onto $SiO_2$ (4 nm)/Si substrate before and after Cl2 plasma exposure for 40, 90, 140 and 220 s. (b) Intensity ratio evolutions of components Si2p (S1), Si2p (S2), Si2p (S4), Si2p (S6) and C1s (Si–C) to C1s (sp2) component as function of plasma treatment duration.

complex reaction is also visible in the Si2p ($S_4$) component. After 60-s plasma exposure time, the intensity ratio of Si2p ($S_2$) and Si2p ($S_6$) to C1s ($sp^2$) increases dramatically and stabilizes from 160-s plasma exposure time. At the same time, the intensity ratio of Si2p ($S_1$), Si2p ($S_4$) and C1s (Si–C) to C1s ($sp^2$) remains unchanged. These observations are attributed to an increase of the $SiO_2$-coated Si nanoparticle signal. Because there is no source of silicon at the surface other than the initial $SiO_2$-coated Si nanoparticle contamination, this observation suggests that the nanoparticles can rearrange and spread on the surface during the plasma treatment.

A similar phenomenon was reported in $H_2$ plasmas, as reported in the TEM image (shown in Supplementary Material). The Si atoms released from nanoparticles during the $H_2$ plasma treatment diffuse at the graphene surface and react with the edges of the 2D PMMA[G] residues where they chemisorb: Silicon is initially spread on the surface but then coalesce again as the PMMA[G] residues are eliminated.[17]

Figure 3 shows the work function map and the corresponding histogram of the sample before (respectively, Fig. 3a and b) and after (respectively, Fig. 3c and d) plasma exposure. The reference exhibits three different work function values (4.4, 4.3 and 4.2 eV)

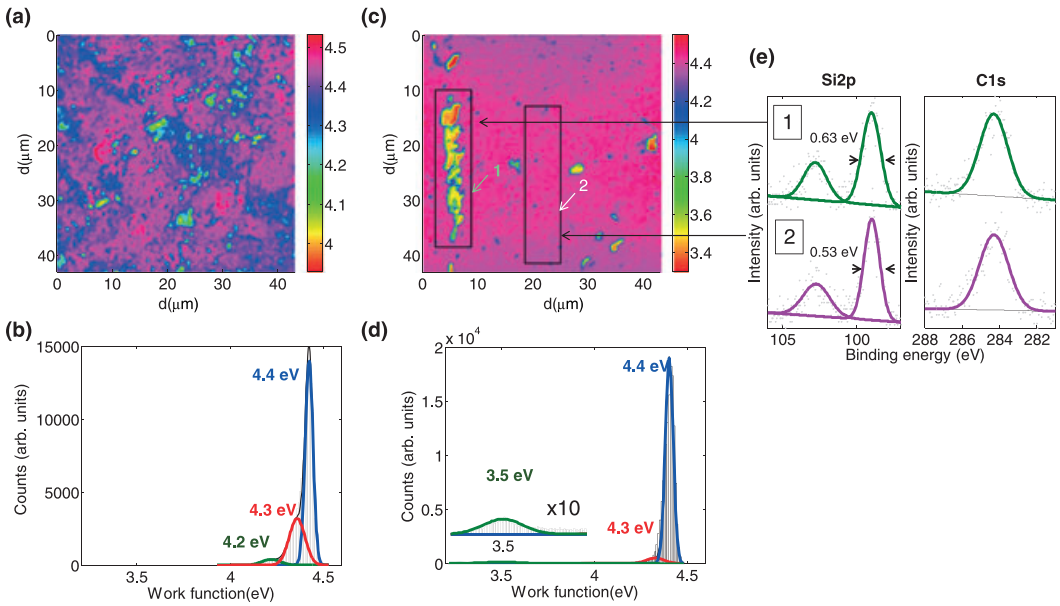


**Figure 3.** Work function map (42 × 42 μm) with the corresponding histogram, respectively, (a) and (b) before and (c) and (d) after $Cl_2$ plasma exposure for 20 s of CVD graphene transferred onto 4-nm-thick $SiO_2$ on Si substrate. Three different work function values attributed to surface chemical heterogeneities are shown. (e) C1s and Si2p core level spectra of two specific regions indicated as 1 and 2 in (c), i.e. after $Cl_2$ plasma treatment for 20 s. The FWHM of the Si2p component depends strongly on the probed region, being much higher in regions of low work function value. All of these analysis were performed by using X-ray source (hν = 1486.8 eV). The typical depth probed by micro-XPS is less than 9 nm in the PMMA (graphene).

attributed to surface chemical heterogeneities. These values do not allow us to specify the nature of the surface chemistry. Figure 3c shows that after a short plasma exposure, the surface is much more homogenous with two main contributions of 4.4 eV and 3.5 eV including one consisting of islands with a very low work function value. To better understand the nature of these islands, we carried out a micro-XPS study of Si2p and C1s core levels, on the island and outside, as shown in Fig. 3e. The obtained C1s core level spectra showed no difference between the two areas. The fitted spectrum to one component provide a peak located at 284.30 eV with a full width at half maximum of 0.75 eV, associated to the presence of graphene. However, the Si2p signature corresponds to different chemical environment from one region to the other because the full width at half maximum of Si2p (Si) peak on and out of the islands is of 630 and 530 meV, respectively. Hence, there is a significant broadening of the Si2p (Si) peak besides the increase of Si2p ($SiO_2$) intensity in the island region, which is indicating that those regions contain Si–$SiO_2$ surface contamination, as reported in previous section. The C1s intensity ratio to the Si2p (Si) does not seem to show a major change but decreases when we take into account the broadening of the Si2p peak (Si: substrate and contamination).

From these results, we can deduce that the surface before treatment shows two types of PMMA residues that correspond to the work function value of 4.3 and 4.4 eV and $SiO_2$-coated Si nanoparticles that correspond to the work function value of 4.2 eV. After plasma treatment, the surface becomes homogeneous with mainly one type of PMMA residues corresponding to the work function value of 4.4 eV (surface area corresponding to 4.3 work function value becomes low). These results show that $Cl_2$ plasma is promising to clean graphene because they have the capability to etch carbonaceous contaminant. Therefore, in good agreement with the previous discussion, these observations suggest that the Si–$SiO_2$ surface contamination that is initially present in the form of nanoparticles (regions with work function = 4.2 eV) is decomposed under the influence of the plasma and then diffuses on the surface where they spread and reorganize (coalesce) to form larger Si–$SiO_2$ islands. This organization explains both a change of the work function value and an increase in area ratio.

## Conclusion

A detailed photoemission study using both laterally averaged and microscopic measurements allowed us to benchmark $Cl_2$ and $H_2$ plasma for graphene cleaning purposes. $H_2$ plasma is efficient to clean PMMA residues but suffers from two drawbacks. Firstly, they do not etch $SiO_2$-coated Si nanoparticle contaminants, and secondly, we have evidence that on graphene reported on $SiO_2$, a liftoff of the graphene layer can take place following the penetration of protons through graphene and their recombination that form a $H_2$ gas between $SiO_2$ and graphene. By contrast, $Cl_2$ plasma is shown to etch slowly PMMA residues without the issue of liftoff ($Cl^+$ ions are too big to pass through the graphene hexagons). However, it induces the decomposition and rearrangement of the $SiO_2$-coated Si nanoparticle contamination that covers the graphene surface and prevents its cleaning. Additional experiments are needed to confirm this conclusion and demonstrate the efficiency of $Cl_2$ plasma to clean.

#### Acknowledgements

The authors thank the French Research Agency through CleanGraph project Nr ANR-13-BS09-0019-04.

The measurements were performed on both the CEA Minatec Nanocharacterization Platform (PFNC) and the clean rooms of CEA-LETI.

## References

[1] A. C. Neto, F. Guinea, N. M. R. Peres, K. S. Novoselov, A. K. Geim, *Rev. Mod. Phys.* **2009**, *81*, 109.
[2] A. Pirkle, J. Chan, A. Venugopal, D. Hinojos, C. W. Magnuson, S. McDonnell, L. Colombo, E. M. Vogel, R. S. Ruoff, R. M. Wallace, *Appl. Phys. Lett.* **2011**, *99*, 122108.
[3] Y. C. Lin, C. C. Lu, C. H. Yeh, C. Jin, K. Suenaga, P. W. Chiu, *Nano Lett.* **2011**, *12*, 414–419.
[4] I. Ruiz, W. Wang, A. George, C. S. Ozkan, M. Ozkan, *Eng. Med.* **2014**, *6* (10), 1070–1075.
[5] G. Algara-Siller, O. Lehtinen, A. Turchanin, U. Kaiser, *Appl. Phys. Lett.* **2014**, *104*, 153115.
[6] M. Her, R. Beams, L. Novotny, *Phys. Lett. A*, **2013**, *377*, 1455.
[7] M. Ishigami, J. H. Chen, W. G. Cullen, M. S. Fuhrer, E. D. Williams, *Nano Lett.* **2007**, *7*, 1643.
[8] C. Gong, H. C. Floresca, D. Hinojos, S. McDonnell, X. Qin, Y. Hao, S. Jandhyala, G. Mordi, J. Kim, L. Colombo, R. S. Ruoff, M. J. Kim, K. Cho, R. M. Wallace, Y. J. Chabal, *J. Phys. Chem. C*, **2013**, *117*, 23000.
[9] H. M. Choi, J. A. Kim, Y. J. Cho, T. Y. Hwang, J. W. Lee, T. S. Kim, *Solid State Phenom.* **2014**, *219*, 68.
[10] K. Kumar, Y. S. Kim, E. H. Yang, *Carbon*, **2013**, *65*, 35.
[11] A. M. Goossens, V. E. Calado, A. Barreiro, K. Watanabe, T. Taniguchi, L. M. K. Vandersypen, *Appl. Phys. Lett.* **2012**, *100*, 073110.
[12] X. Liang, B. A. Sperling, I. Calizo, G. Cheng, C. A. Hacker, Q. Zhang, Y. Obeng, K. Yan, H. Peng, Q. Li, X. Zhu, H. Yuan, A. R. H. Walker, Z. Liu, L. Peng, C. A. Richter, *ACS Nano*, **2011**, *5*, 9144.
[13] N. Peltekis, S. Kumar, N. McEvoy, K. Lee, A. Weidlich, G. S. Duesberg, *Carbon*, **2012**, *50*, 395.
[14] N. McEvoy, H. Nolan, N. A. Kumar, T. Hallam, G. S. Duesberg, *Carbon*, **2013**, *54*, 283.
[15] Y. D. Lim, D. Y. Lee, T. Z. Shen, C. H. Ra, J. Y. Choi, W. J. Yoo, *ACS Nano*, **2012**, *6*, 4410.
[16] S. Grenadier, J. Li, J. Lin, H. Jiang, *J. Vac. Sci. Tech. A*, **2013**, *31*, 061517.
[17] G. Cunge, D. Ferrah, C. Petit-Etienne, A. Davydova, H. Okuno, D. Kalita, V. Bouchiat, O. Renault, *J. Appl. Phys.* **2015**, *118*, 123302.
[18] X. Zhang, T. Schiros, D. Nordlund, Y. C. Shin, J. Kong, M. Dresselhaus, T. Palacios, *Adv. Funct. Mater.* **2015**, *25*, 4163.
[19] M. Darnon, C. Petit-Etienne, E. Pargon, G. Cunge, L. Vallier, P. Bodart, M. Haas, S. Banna, T. Lill, O. Joubert, *ECS Trans.* **2010**, *27*, 717.
[20] G. Cunge, B. Pelissier, O. Joubert, R. Ramos, C. Maurice, *Plasma Sources Sci. Technol.* **2005**, *14*, 599.
[21] R. F. Roberts, D. L. Allara, C. A. Pryde, D. N. E. Buchanan, N. D. Hobbins, *Surf. Interface Anal.* **1980**, *2*, 5.
[22] S. Unarunotai, Y. Murata, C. E. Chialvo, H. S. Kim, S. MacLaren, N. Mason, I. Petrov, J. A. Rogers, *Appl. Phys. Lett.* **2009**, *95*, 202101.
[23] M. Escher, K. Winkler, O. Renault, N. Barrett, *J. Electron Spectrosc. Relat. Phenom.* **2010**, *178*, 303.
[24] A. Barinov, L. Gregoratti, P. Dudin, S. La Rosa, M. Kiskinova, *Adv. Mater.* **2009**, *21*, 1916.
[25] E. Despiau-Pujo, A. Davydova, G. Cunge, L. Delfour, L. Magaud, D. B. Graves, *J. Appl. Phys.* **2013**, *113*, 114302.
[26] A. Davydova-Pujo, MD simulation of $H_2$ plasma/ graphene interaction for innovative etching processes development, PhD thesis. University of Grenoble, **2014**.
[27] G. Hollinger, F. J. Himpsel, *Appl. Phys. Lett.* **1984**, *44*, 93.

## Supporting Information

Additional supporting information may be found in the online version of this article at the publisher's web site.